THE ASTROPHYSICAL JOURNAL, 513:383–400, 1999 March 01


# RELATIVISTIC AND NEWTONIAN CORE-SHELL MODELS: ANALYTICAL AND NUMERICAL RESULTS

WERNER M. VIEIRA AND PATRICIO S. LETELIER
Departamento de Matemática Aplicada, Instituto de Matemática, Estatística e Computação Científica, Universidade Estadual de Campinas, CP 6065, 13081-970 Campinas, SP, Brazil; vieira@ime.unicamp.br, letelier@ime.unicamp.br
*Received 1998 July 17; accepted 1998 September 12*

## ABSTRACT

We make a detailed analysis of the exact relativistic core-shell models recently proposed to describe a black hole or neutron star surrounded by an axially symmetric, hollow halo of matter and in a seminal sense also galaxies, since there are massive shell-like structures—as, for example, rings and shells—surrounding many of them and also evidence for many galactic nuclei hiding black holes. We discuss the unicity of the models in relation to their analyticity at the black hole horizon and to the full elimination of axial (conical) singularities. We also consider Newtonian and linearized core-shell models, on their own to account for dust shells and rings around galaxies and supernovae and star remnants around their centers, and also as limiting cases of the corresponding relativistic models to gain physical insight. Second, these models are generic enough to numerically study the role played by the presence/lack of *discrete* reflection symmetries about planes, i.e., the presence/lack of equatorial planes, in the chaotic behavior of the orbits. This is to be contrasted with the almost universal acceptance of reflection symmetries as default assumptions in galactic modeling. We also compare the related effects if we change a true central black hole by a Newtonian central mass. Our main numerical findings are as follows: (1) The *breakdown* of the reflection symmetry about the equatorial plane in both Newtonian and relativistic core-shell models (a) *enhances* in a significant way the chaotic behavior of orbits in reflection symmetric *oblate* shell models and (b) *inhibits* significantly also the occurrence of chaos in reflection symmetric *prolate* shell models. In particular, in the prolate case the lack of the reflection symmetry provides the phase space with a robust family of regular orbits that is otherwise not found at higher energies. (2) The relative extents of the chaotic regions in the relativistic cases (i.e., with a true central black hole) are significantly larger than in the corresponding Newtonian ones (which have just a $-1/r$ central potential).

*Subject headings:* black hole physics — circumstellar matter — galaxies: structure — relativity — stars: neutron

## 1. INTRODUCTION

We make a more detailed study, both analytical and numerical, of some *exact relativistic* solutions we recently proposed to describe static, axially symmetric massive core-shell systems (Vieira & Letelier 1996a, 1997, hereafter VL1 and VL2, respectively). We add in this way to the efforts of modeling many situations of interest in astrophysics involving massive shell-like structures around centers, as, for example, black holes or neutron stars surrounded by massive shell and ring remnants. A nice illustration of this possibility is offered by the famous Supernova 1987A plus its physical rings; see, e.g., Panagia et al. (1996), Meyer (1997) and Chevalier (1997). At least in a seminal sense, the model could also describe galaxies, since there are many of them that exhibit massive rings (Sackett & Sparke 1990; Arnaboldi et al. 1993; Reshetnikov & Sotnikova 1997) and shells (Malin & Carter 1983; Quinn 1984; Dupraz & Combes 1987; Barnes & Hernquist 1992), whereas many others possibly have galactic nuclei hiding black holes (see Kormendy & Richstone 1995 for a review).

Specifically, we implement here a monopolar core (a black hole in the relativistic case) plus an exterior shell of dipoles, quadrupoles, and octopoles. Obviously, these multipoles are shell-like Legendre expansions, i.e., their corresponding terms increase with the distance in the intermediate vacuum between the core and the shell. Beyond its own applicability, the model also points to the possibility of a realistic description of any axially symmetric relativistic core-shell configuration whose approximation as a static system should be valid at some useful timescale, via a systematic multipolar Legendre expansion. In fact, a further step in this program was finally started in Letelier & Vieira (1997) by giving stationarity (rotation) to the relativistic case of a monopolar core plus a purely dipolar shell. This is an important improvement, since real celestial objects do rotate. The present analysis will be extended to rotating core-shell models in a forthcoming contribution.

Additionally, we consider the Newtonian counterpart of the relativistic model above, which was only sketched in the previous works, and show that they could describe core-shell systems "per se" interesting in astronomy. So, we can have massive circumstellar dust shells around certain types of stars as by-products of their death; see, e.g., Barlow et al. (1994) for an example of (irregular) circumstellar shells around luminous blue variables and a review by Groenewegen et al. (1998) about dust shells around carbon Mira variables. Another potential application for core-shell models is to the more speculative possibility of hollow galactic halos of dark matter made of neutrinos recently considered by Ralston & Smith (1991), Madsen (1991), and Barnes (1993). Moreover, we will see that the study of the relativistic core-shell model in parallel to its Newtonian counterpart is useful also to clarify the physical content of the former one.

After Poincaré (1957) and the KAM theory (after Kolmogorov 1954; Arnol'd 1963a, 1963b; Moser 1967) it became well established that nonintegrability and hence chaos is a general rather than exceptional manifestation in the context of dynamical systems (whether or not physical applications are concerned) (see Berry 1978). Given this ubiquitous fact, an

important issue in astronomical modeling is to study which extent in phase space chaotic behavior rises in models that are relevant to describe real systems and what its consequences are. For example, Binney (1982a) discusses the difficulties of constructing stationary self-consistent models when a significant fraction of orbits is irregular, since they may not obey either Vlasov's or Jean's equations. Then, it is remarkable that a wide class of fully integrable potentials, the so-called Stäckel potentials (Lynden-Bell 1962; de Zeeuw 1985; de Zeeuw, Peletier, & Franx 1986), are feasible starting points to describe, by themselves or by adding perturbations, real disk, elliptical, or even triaxial galaxies. For more realistic tridimensional models there is evidence for rounder and smoother mass distributions generating only relatively small fractions of chaotic orbits (Schwarzschild 1979; Binney & Tremaine 1987; Evans, Häfner, & de Zeeuw 1997), whereas flattening and/or sharpening of the mass distributions, for example, through increasing triaxiality and/or putting cusps and central masses to mimic black holes, tends to increase the chaotic behavior and force us to take it into account (Gerhard & Binney 1985; Schwarzschild 1993; Merritt & Fridman 1996; Norman, Sellwood, & Hasan 1996; Merritt 1997; Valluri & Merritt 1998). On the other hand, the emergence of chaos in two-dimensional models has more loose correlations with morphological aspects; see, for example, Binney & Spergel (1982), Richstone (1982), Binney (1982b), Gerhard (1985), and Sridhar & Touma (1997).

We address in this work also a numerical study about the chaotic behavior of orbits trapped in the bound gravitational zones between the core and the external massive shell. Beyond its own applicability as seen above, we take advantage of models that are generic within the class of axially symmetric core-shell distributions and, moreover, offer exact relativistic and Newtonian counterparts to be compared, in order to achieve some understanding about chaotic behavior related to two aspects: first to the role of reflection symmetries shared by almost all models in astronomy and astrophysics and second to the consequences of treating exact central black holes as just Newtonian central masses.

In the first part of this article (§ 2) we present analytical results concerning some properties like unicity and analyticity of the relativistic solutions themselves, in connection with both the linearized core-shell solutions and the corresponding Newtonian models taken as limiting cases.

In § 2.1 we enlarge the relativistic solution presented in VL1 for a monopolar core plus a shell of quadrupoles and octopoles in order to include a dipolar shell component. This complete solution was only outlined in VL2. In this latter reference it was emphasized that the case of a core plus purely dipolar shell is physically nontrivial already in the Newtonian gravity; moreover, it was shown that the Newtonian dipolar case is integrable, in contrast with its chaotic relativistic counterpart, which allowed us to characterize the chaotic behavior in this case as an intrinsic general relativistic effect. Here, we take advantage of this striking difference of the dipolar case in order to reinforce the numerical conclusions presented in § 3 concerning the nontrivial dynamical role played by the presence/absence of the *discrete* reflection symmetry about the equatorial plane on the chaotic behavior of the orbits.

In § 2.2 we proceed to a full elimination of axial (conical) singularities (CSs) from the relativistic model, which was only partially accomplished in VL1. In fact, CSs are not globally removable from either static or stationary many-body relativistic solutions, since they are self-consistently demanded by Einstein's equations to strut the otherwise unstable configuration against its own gravity (see Robertson & Noonan 1968 and Letelier & Oliveira 1998 for a recent review). So, in the present case the most we can do is really move them all outside the shell, thus obtaining a true vacuum in the intermediate space between the core and the shell. We also discuss in this section the conditions for the Kruskal-type analyticity of the solutions at the horizon of the central black hole and use both aspects to find the conditions under which the unicity of the models is assured.

In § 2.3 we present the linearization of the relativistic model in the multipole strengths via the so-called Regge-Wheeler (RW) formalism. In particular, we see that our model exemplifies the fact that CSs survive to the linearization process, their presence in the intermediate vacuum being in fact an obstruction to the application of the RW formalism. This reinforces the interpretation of CSs as a kind of singular matter distribution necessary to the dynamical consistency of static and stationary relativistic models. In spite of being intrinsically relativistic manifestations, an adiabatic treatment of CSs in the Newtonian limit allows for estimates concerning the emission rate of gravitational waves by two coalescing rotating black holes (Araujo, Letelier, & Oliveira 1998).

In § 2.4 we discuss Newtonian core-shell models, on their own, as well as limiting cases of the corresponding relativistic ones. We put the Hénon-Heiles–like structure of the relativistic models in the appropriate astronomical context and stress the physical content of the various terms present in them; in particular we see that the apparently naive constant relativistic solution does in fact hide a relativistic homoeoid (see Chandrasekhar 1987 for Newtonian homoeoids).

The numerical part of this article is presented in § 3 and deals with a study of the chaotic behavior of orbits trapped in the intermediate vacuum between the core and the shell. Specifically, we shall explore in this section the fact that, due to its generality, axially symmetric core-shell expansions are particularly suitable to study the dynamical role played by a discrete symmetry of the model, namely, the reflection symmetry about an equatorial plane, on the chaotic behavior of orbits. The reflection symmetry is present in the model if and only if the shell is of even type, i.e., if and only if $2^{2n}$-poles, $n = 0, 1, 2, 3, \ldots$, occur in the shell expansion, and it is broken if we add any odd, $2^{2n+1}$-poles to the expansion. The hypothesis of reflection symmetry is a widely spread assumption in astronomical modeling, and its twofold justification lies primarily in that too many real celestial objects to be modeled—for example, stars themselves, star clusters, and galaxies—seem in fact very symmetric with respect to a middle plane. Another reason for this symmetry assumption is that the resulting model gets strongly simplified in both analytical and numerical aspects. Of course, we do not expect the reflection symmetry be realized in nature exactly, so it is relevant to search for possible detectable dynamical effects arising from deviations of that symmetry.

A strong additional motivation for this numerical study is to compare from the point of view of the chaotic behavior what happens when the presence of true central black holes is simplified by reducing them to Newtonian central masses. This is a common practice in current modeling, as, for example, in Gerhard & Binney (1985), Sridhar & Touma (1997), and Valluri & Merritt (1998).

Surprisingly enough, the numerical findings show marked effects on the chaotic behavior of the orbits in the intermediate vacuum between the core and the shell linked to the presence/lack of the reflection symmetry in the relativistic, as well as Newtonian, models. We also find strong quantitative differences in the chaotic behavior manifested in both relativistic and Newtonian cases.

Finally, we present the conclusions with some discussion and prospects in § 4.

## 2. ANALYTICAL RESULTS: EXACT, LINEARIZED, AND NEWTONIAN CORE-SHELL MODELS

### 2.1. *The Exact Model*

We deal here with static, axially symmetric models, for which the Weyl coordinates $(t, \rho, z, \phi)$ are the starting point:

$$ds^2 = e^{2v}\,dt^2 - e^{2\gamma-2v}[dz^2 + d\rho^2] - e^{-2v}\rho^2\,d\phi^2\ , \tag{1}$$

where $v$ and $\gamma$ are functions of $\rho$ and $z$ only. Except where units are explicitly required (particularly in § 2.4), we use nondimensional variables: $s \leftrightarrow s/L$ (idem for $\rho$ and $z$), and $t \leftrightarrow ct/L$ where $c$ is the light velocity in vacuum and $L$ is some convenient unit of length. Einstein's equations in absence of matter (vacuum) reduce in this case to the usual Laplace equation for $v$

$$v_{,\rho\rho} + \frac{1}{\rho}\,v_{,\rho} + v_{,zz} = 0\ , \tag{2}$$

and the quadrature

$$d\gamma = \rho[(v_{,\rho})^2 - (v_{,z})^2]d\rho + 2\rho v_{,\rho}\,v_{,z}\,dz \tag{3}$$

for $\gamma$.

Before proceeding, we mention that the Weyl coordinates should be considered somewhat deceiving if we insist in naively transferring their image contents about mass configurations to the Newtonian common sense. For example, the spherical shape of the horizon of a black hole is compressed into a bar in Weyl's coordinates, the interior portion of the black hole spacetime being wholly discarded from the portrait. Apart from the well-known fact that the relativistic context is not cast in a straight relation with the Newtonian one in strong regimes, they are mathematically sound, as will be clear later when we will compare both versions of the core-shell models.

We pass to the prolate spheroidal coordinates $(t, u, v, \phi)$, which have a direct link with the "spherical" ones $(t, R, \theta, \phi)$ $(R \leftrightarrow R/L)$ we will use later,

$$\begin{aligned} u &= R - 1 = \tfrac{1}{2}[\sqrt{\rho^2 + (z+1)^2} + \sqrt{\rho^2 + (z-1)^2}]\ , \quad u \geq 1\ , \\ v &= \cos\,\theta = \tfrac{1}{2}[\sqrt{\rho^2 + (z+1)^2} - \sqrt{\rho^2 + (z-1)^2}]\ , \quad -1 \leq v \leq 1\ , \end{aligned} \tag{4}$$

or, in terms of $\rho$, $z$,

$$\begin{aligned} \rho &= \sqrt{(u^2-1)(1-v^2)} = \sqrt{R(R-2)}\,\sin\,\theta\ , \quad R \geq 2\ , \\ z &= uv = (R-1)\,\cos\,\theta\ . \end{aligned} \tag{5}$$

Equations (2) and (3) are written in terms of $u$, $v$ as

$$[(u^2-1)v_{,u}]_{,u} + [(1-v^2)v_{,v}]_{,v} = 0\ , \tag{6}$$

$$\gamma_{,u} = \frac{1-v^2}{u^2-v^2}\,[u(u^2-1)(v_{,u})^2 - u(1-v^2)(v_{,v})^2 - 2v(u^2-1)v_{,u}\,v_{,v}]\ ,$$

$$\gamma_{,v} = \frac{u^2-1}{u^2-v^2}\,[v(u^2-1)(v_{,u})^2 - v(1-v^2)(v_{,v})^2 + 2u(1-v^2)v_{,u}\,v_{,v}]\ . \tag{7}$$

In the prolate spheroidal coordinates $u$, $v$, Laplace equation (6) can be separated and solved in terms of standard Legendre polynomials $Q_\ell$,$P_\ell$ (see, for example, Moon & Spencer 1988, and, for relativistic applications, Reina & Treves 1976):

$$v(u, v) = \ell = \sum_0^\infty\,[a_\ell\,Q_\ell(u) + b_\ell\,P_\ell(u)][c_\ell\,Q_\ell(v) + d_\ell\,P_\ell(v)]\ . \tag{8}$$

The particular solution picked out from the general one above is determined by the matter distribution whose model is wanted. We are interested here in monopolar core plus shell-type models, so we are guided by the Newtonian case (to be detailed in § 2.4) to the specific solution of the form (up to third order)

$$2v = 2v_0 - 2\kappa Q_0(u) + 2\mathscr{D}P_1(u)P_1(v) + \tfrac{4}{3}\mathscr{Q}P_2(u)P_2(v) + \tfrac{4}{5}\mathscr{O}P_3(u)P_3(v)\ . \tag{9}$$

The coordinate $v_0$ is an integration constant and $Q_0$ describes the monopolar core, which either reduces to a black hole if we set $\kappa = 1$ and identify $2L$ with the Schwarzschild radius of the core [in which case $(t, R, \theta, \phi)$ above are Schwarzschild's coordinates] or can be switched off by simply setting $\kappa = 0$. The remaining terms correspond to the multipoles that originated from the exterior shell of matter: dipole $\mathscr{D}$, quadrupole $\mathscr{Q}$, and octopole $\mathscr{O}$ (note the opposite sign convention for dipoles in this definition with respect to that appearing in VL2). The nontrivial character of shell dipoles in both Newtonian and general relativistic theories of gravity has been anticipated in VL2, whereas shells made of quadrupoles plus octopoles were con-

sidered in VL1. If nonmonopolar cores should be considered, we should add to equation (9) terms of the form $Q_\ell(u)P_\ell(v)$, $\ell \geq 1$.

Much more sophisticated multipolar relativistic treatments for core, shell, and core-shell models are considered by Thorne (1980), Zhang (1986), and Suen (1986a, 1986b), respectively, in terms of higher order systematic expansions of the metric in de Donder coordinates. Our approach is more modest at this stage and inspired only on the zeroth order, Newtonian limit of the full relativistic situation.

The odd multipoles of $v$ in equation (9) ($\mathscr{D}$ and $\mathscr{O}$ in the present case) break the reflection symmetry about the plane $z = 0$, and we shall show in § 2.2 that we need both $\mathscr{D}$ and $\mathscr{O}$ to be simultaneously either present or absent if we want to rule out conical singularities of the intermediate vacuum between the core and the shell. We rewrite equation (9) as

$$2v = \kappa \log\left(\frac{u-1}{u+1}\right) + P(u, v) ,$$

$$P = 2v_0 + 2\mathscr{D}uv + \frac{1}{3}\mathscr{Q}(3u^2 - 1)(3v^2 - 1) + \frac{1}{5}\mathscr{O}uv(5u^2 - 3)(5v^2 - 3) . \tag{10}$$

After integrating equation (7) we obtain the corresponding solution for $\gamma$:

$$2\gamma = \kappa^2 \log\left(\frac{u^2-1}{u^2-v^2}\right) + Q(u, v) ,$$

$$Q = 2\gamma_0 + \gamma_D + \gamma_Q + \gamma_O + \gamma_{DQ} + \gamma_{DO} + \gamma_{QO} ,$$

$$\gamma_D = 4\kappa\mathscr{D}v - \mathscr{D}^2[u^2(1 - v^2) + v^2] ,$$

$$\gamma_Q = -4\kappa\mathscr{Q}u(1 - v^2) + \frac{1}{2}\mathscr{Q}^2[u^4(1 - v^2)(1 - 9v^2) - 2u^2(1 - v^2)(1 - 5v^2) - v^2(2 - v^2)] ,$$

$$\gamma_O = -\frac{2}{5}\kappa\mathscr{O}v[5(3u^2 - 1)(1 - v^2) - 4] + \frac{3}{100}\mathscr{O}^2[-25u^6(1 - v^2)(5v^2 + 2v - 1)(5v^2 - 2v - 1)$$
$$+ 15u^4(1 - v^2)(65v^4 - 40v^2 + 3) - 3u^2(1 - v^2)(25v^2 - 3)(5v^2 - 3) - v^2(25v^4 - 45v^2 + 27)] ,$$

$$\gamma_{DQ} = -4\mathscr{D}\mathscr{Q}uv(u^2 - 1)(1 - v^2) ,$$

$$\gamma_{DO} = \frac{3}{10}\mathscr{D}\mathscr{O}[u^2(5u^2 - 6)(1 - v^2)(1 - 5v^2) + v^2(5v^2 - 6)] ,$$

$$\gamma_{QO} = -\frac{6}{5}\mathscr{Q}\mathscr{O}uv(u^2 - 1)(1 - v^2)[(5u^2 - 1)(3v^2 - 1) + 2(1 - v^2)] . \tag{11}$$

This is the complete solution, which was outlined in VL2. The additional integration constant $\gamma_0$ will be fixed in the next section in connection with the elimination of conical singularities from the intermediate vacuum, whereas the integration constant $v_0$ will prove to be necessary in assuring analyticity to the full core-shell solution at the horizon in the absence of conical singularities. The terms proportional to $\kappa$ in $\gamma_D$, $\gamma_Q$, and $\gamma_O$ represent nonlinear interactions between the black hole and the external shell.

### 2.2. *Unicity and Smoothness Requirements*

We shall be interested in two classes of singularities of the Weyl spacetime. The first one is the strong singularities that are located in the points wherein the scalar polynomial invariants of the curvature tensor blow up. For a static axially symmetric spacetime solution to the vacuum field equations we have only two nonvanishing invariants. They are (Carminati & McLenaghan 1991) $w_1 \equiv \frac{1}{8}C_{abcd}C^{abcd}$ and $w_2 \equiv -\frac{1}{16}C^{cd}_{ab}C^{ef}_{cd}C^{ab}_{ef}$ where $C^{abcd}$ is the Weyl trace-free tensor, which for vacuum solutions coincides with the Riemann curvature tensor. After some algebraic manipulations, they reduce to

$$w_1 = 2\kappa^2\{3\sigma(v_{,z}^2 + \rho^2 v_{,\rho}^2 v_{,z}^2 - v_{,\rho}/\rho - \rho v_{,\rho}\sigma) + v_{,\rho}^2(1 + 2\rho\gamma_{,\rho} + 3\rho v_{,\rho}) + \rho^2(v_{,z}^6 + v_{,\rho}^6)$$
$$+ v_{,\rho z}[6v_{,\rho}v_{,z} + v_{,\rho z} - 2(v_{,z}\gamma_{,\rho} + v_{,\rho}\gamma_{,z})] + v_{,\rho\rho}[3\gamma_{,\rho}(1 - 2\rho v_{,\rho})/\rho - v_{,zz} + 2v_{,z}\gamma_{,z}]\} ,$$
$$w_2 = 3\kappa^3\rho^{-2}(v_{,\rho}/\rho - \sigma)(\sigma[3\rho^3 v_{,\rho}^2 v_{,z}^2 + \rho(1 - 3\rho v_{,\rho})\sigma + 2v_{,\rho}] - v_{,z}^2[\gamma_{,\rho} + 3v_{,\rho}(1 - 2\rho v_{,\rho})]$$
$$+ \rho^3(v_{,z}^6 + v_{,\rho}^6) + rv_{,\rho z}\{2v_{,z}[3v_{,\rho}(1 - \rho v_{,\rho}) + \rho v_{,z}^2] + v_{\rho z}\} + v_{,\rho\rho}[3\gamma_{,\rho}(1 - 2\rho v_{,\rho}) + 4\rho^2 v_{,\rho}^3 - \rho v_{,zz}]) , \tag{12}$$

where $\sigma \equiv v_{,z}^2 + v_{,\rho}^2$ and $\kappa \equiv \exp 2(v - \gamma)$. In the present case, these scalars are singular on the position of the attraction center and will also be singular in some directions of the spatial infinity (the specific directions will depend on the signs of $\mathscr{D}$, $\mathscr{Q}$, etc.), in other words they are singular in the position of the sources of the gravitational field.

There is another class of singularities that does not show up in a simple way in the curvature, the so-called conical singularities (CSs) (Sokolov & Starobinskii 1977). These singularities are in some sense like the distributions related to a low-dimensional Newtonian potential, e.g., for an infinite massive wire the potential is $\phi = 2\lambda \log \rho$, we have that the Laplace equation, the analog to the curvature, gives us $\nabla^2\phi = 0$ for $\rho \neq 0$, whereas for $\rho = 0$ we need to use some global property, for example, Gauss theorem, to get $\nabla^2\phi = 4\pi\lambda\delta(\rho)$. To be more precise, let us consider a conical surface, $z = \alpha\rho$, embedded in the

usual Euclidean three-dimensional space $ds^2 = d\rho^2 + \rho^2\, d\varphi^2 + dz^2$, so that we have on the cone $ds^2 = (1+\alpha^2)d\rho^2 + \rho^2\, d\varphi^2 = d\bar{\rho}^2 + \beta^2\bar{\rho}^2\, d\bar{\varphi}^2$ with $\bar{\rho} = (1+\alpha^2)^{1/2}\rho$ and $\beta^2 = 1/(1+\alpha^2)$. Note that the coordinate range of $\bar{\rho}$, as well as that of $\varphi$, is the usual one. The ratio between the arc of the circumference and its radius is $2\beta\pi$ in this case. If we compute the Riemann tensor for this last metric we find that $R_{\bar{\rho}\varphi\bar{\rho}\varphi} = 0$ for $\bar{\rho} \neq 0$. By using the Gauss-Bonnet theorem in this case, we can pick up the curvature singularity as being of the form $R_{\bar{\rho}\varphi\bar{\rho}\varphi} \propto \delta(\bar{\rho})$.

It is well known that CSs arise when we consider Weyl's solutions near the symmetry axis (Robertson & Noonan 1968 and Letelier & Oliveira 1998). They are interpreted as a geometric consequence of the presence of some kind of "strut," necessary to consistently prevent any static nonspherically symmetric model from collapsing due to self-gravity. In this sense, the uniqueness of the core-type, one-body solution for the (static) spherically symmetric Einstein's equation (namely, the Schwarzschild one) should relate to the fact that it is impossible to attach struts in a perfectly round metric. For the Weyl solutions, we can always consider a small disk centered in the symmetry axis ($t = t_0$, $z = z_0$, $\rho = \epsilon$, $0 \leq \varphi < 2\pi$) and require that the ratio between the circumference and its radius equals $2\pi$. This is the condition to eliminate CSs from the intermediate vacuum (then attaching them to infinity), which amounts to imposing the well-known conditions of elementary flatness on the function $\gamma$

$$2\gamma\Big|_{\rho=0,\,|z|>1} \equiv 2\gamma\Big|_{u=|z|,\,v=\pm 1} = 0\,. \tag{13}$$

These two conditions fix the constant $\gamma_0$ and impose an additional constraint on the *odd* shell multipoles ($\mathscr{D}$ and $\mathscr{O}$ here) in the presence of the black hole:

$$2\gamma_0 - \mathscr{D}^2 - \tfrac{1}{2}\mathscr{Q}^2 - \tfrac{21}{100}\mathscr{O}^2 - \tfrac{3}{10}\mathscr{D}\mathscr{O} = 0\,, \tag{14}$$

$$\kappa[\mathscr{D} + \tfrac{2}{5}\mathscr{O}] = 0\,. \tag{15}$$

The condition (14) fixing $\gamma_0$ is necessary in all cases to rule out the conical singularities. From equation (15) we see that the former is also a sufficient condition in two cases: (1) the shell of dust is left alone by switching off the core ($\kappa = 0$), and (2) in the presence of the black hole ($\kappa = 1$), the shell is made only of even-type multipoles ($\mathscr{Q}$ here). We also see that it is possible to eliminate conical singularities for a single or pure shell component only if it is of the even type. Then, it follows that the core-shell dipole solution presented in VL1, as well as those with $\mathscr{O} \neq 0$ presented in VL2, all have conical singularities since they do satisfy equation (14) but *not* equation (15). If we include the necessary condition (14) in equation (11), we have the following for $\gamma$:

$$\begin{aligned}
2\gamma &= \kappa^2 \log\left(\frac{u^2-1}{u^2-v^2}\right) + Q(u, v)\,,\\
Q &= \gamma_D + \gamma_Q + \gamma_O + \gamma_{DQ} + \gamma_{DO} + \gamma_{QO}\,,\\
\gamma_D &= 4\kappa\mathscr{D}v - \mathscr{D}^2(u^2-1)(1-v^2)\,,\\
\gamma_Q &= -4\kappa\mathscr{Q}u(1-v^2) - \frac{1}{2}\mathscr{Q}^2(u^2-1)(1-v^2)[u^2(9v^2-1)+1-v^2]\,,\\
\gamma_O &= -\frac{2}{5}\kappa\mathscr{O}v[5(3u^2-1)(1-v^2)-4] - \frac{3}{100}\mathscr{O}^2(u^2-1)(1-v^2)[(25u^4-20u^2+1)(25v^4-14v^2+1)\\
&\quad + 30u^2v^2(5v^2-1) + 6(1-v^2)]\,,\\
\gamma_{DQ} &= -4\mathscr{D}\mathscr{Q}uv(u^2-1)(1-v^2)\,,\\
\gamma_{DO} &= \frac{3}{10}\mathscr{D}\mathscr{O}(u^2-1)(5u^2-1)(1-v^2)(1-5v^2)\,,\\
\gamma_{QO} &= -\frac{6}{5}\mathscr{Q}\mathscr{O}uv(u^2-1)(1-v^2)[(5u^2-1)(3v^2-1)+2(1-v^2)]\,.
\end{aligned} \tag{16}$$

Here, it is explicitly seen that only the first terms in $\gamma_D$ and $\gamma_O$, respectively, do not vanish identically at $v = \pm 1$. They cancel one another at those points only if we use the additional condition (15) in the equation above, which amounts to putting there either $\kappa = 0$ or $\mathscr{D} + \frac{2}{5}\mathscr{O} = 0$ plus $\kappa = 1$. In the latter case, $\gamma$ finally becomes

$$\begin{aligned}
2\gamma &= \log\left(\frac{u^2-1}{u^2-v^2}\right) + Q(u, v)\,,\\
Q &= \gamma_Q + \gamma_{DO} + \gamma_{QDO}\,,\\
\gamma_Q &= -4\mathscr{Q}u(1-v^2) - \frac{1}{2}\mathscr{Q}^2(u^2-1)(1-v^2)[u^2(9v^2-1)+1-v^2]\,,\\
\gamma_{DO} &= -2\mathscr{O}v(3u^2-1)(1-v^2) - \frac{1}{4}\mathscr{O}^2(u^2-1)(1-v^2)(75u^4v^4 - 42u^4v^2 - 42u^2v^4 + 18u^2v^2 + 3u^4 + 3v^4 + 1)\,,\\
\gamma_{QDO} &= -2\mathscr{Q}\mathscr{O}uv(u^2-1)(1-v^2)(3u^2-1)(3v^2-1)\,,
\end{aligned} \tag{17}$$

if we remember that now $\mathscr{D}$ is present only through $\mathscr{O}$.

An arbitrariness remains in the full solution, namely, the constant $v_0$. To show that it plays a nontrivial role in assuring analyticity to the solution at the black hole horizon, we start by writing the solution in the Schwarzschild coordinates $(t, R, \theta, \phi)$:

$$ds^2 = \left(1 - \frac{2}{R}\right)e^P dt^2 - e^{Q-P}\left[\left(1 - \frac{2}{R}\right)^{-1} dR^2 + R^2 d\theta^2\right] - e^{-P}R^2 \sin^2\theta\, d\phi^2 , \tag{18}$$

with $P = P(u = R - 1, v = \cos\theta)$ and $Q = Q(u = R - 1, v = \cos\theta)$ given, respectively, by equations (10) and (11) with $\kappa = 1$. At first sight we should expect that the singularity of this metric at the horizon remains only a coordinate defect, since all metric functions here differ from the corresponding Schwarzschild ones by well-behaved exponentials. To see what really happens there, we go to Kruskal coordinates $(V, U, \theta, \phi)$, defined as

$$(R - 2)e^{R/2} = U^2 - V^2 ,$$
$$t = 2\log\left(\frac{U + V}{U - V}\right), \tag{19}$$

in order to eliminate the usual horizon divergence coming from the factor $(1 - 2/R)^{-1}$. The new, Kruskal components $g'_{\mu\nu}(x')$ are obtained from the old, Schwarzschild ones $g_{\alpha\beta}(x)$ via

$$g'_{\mu\nu}(x') = \frac{\partial x^\alpha}{\partial x'^\mu}\frac{\partial x^\beta}{\partial x'^\nu} g_{\alpha\beta}(x) . \tag{20}$$

The line element (18) reads in Kruskal's coordinates as

$$ds^2 = F^2[-(1 - HU^2)dU^2 + (1 + HV^2)dV^2] - e^{Q-P}R^2 d\theta^2 - e^{-P}R^2 \sin^2\theta\, d\phi^2 , \tag{21}$$

where $R$ (and hence $u = R - 1$) is implicitly, analytically given in terms of $U, V$ by the first relation in equation (19), $v = \cos\theta$, and $F^2$ and $H$ are defined by

$$F^2 \equiv \frac{16}{R} e^{-R/2}e^P ,$$
$$H \equiv (1 - e^{Q-2P})(U^2 - V^2)^{-1} . \tag{22}$$

An inspection of equations (21) and (22) clearly shows that this metric is analytic at the horizon ($u = R - 1 = 1$ or $U = \pm V$) if and only if $H$ is analytic there. If we define $u = R - 1 = 1 + \epsilon$, from which it follows that $U^2 - V^2 = \epsilon\, e^{(1+\epsilon/2)}$, this amounts just to imposing the finiteness of $\lim_{\epsilon\to 0} H$. In fact, we see that $Q - 2P = C_0 + f(\cos\theta)\epsilon + O(\epsilon^2)$, with $C_0$ a constant depending only upon $v_0, \gamma_0, \mathscr{D}, \mathscr{Q}$, and $\mathscr{O}$, and $f$ being a function only of $\cos\theta$, so that the limit

$$\lim_{\epsilon\to 0} H = \lim_{\epsilon\to 0}\left\{e^{-(1+\epsilon/2)}\left[\frac{(1 - e^{C_0})}{\epsilon} - e^{C_0}f(\cos\theta) + O(\epsilon)\right]\right\} \tag{23}$$

is finite [and equals to $-e^{-1}f(\cos\theta)$] if and only if the condition $C_0 = 0$ holds identically. This additional constraint on $v_0$ and $\gamma_0$ reads

$$-2(2v_0 + \tfrac{4}{3}\mathscr{Q}) + [2\gamma_0 - \mathscr{D}^2 - \tfrac{1}{2}\mathscr{Q}^2 - \tfrac{21}{100}\mathscr{O}^2 - \tfrac{3}{10}\mathscr{D}\mathscr{O}] = 0 , \tag{24}$$

which fixes $v_0$. We see that the analyticity at the horizon and the nonexistence of conical singularities are independent conditions; however, if the necessary condition for the absence of conical singularities (14) also holds, equation (24) reduces to the following first-order relation

$$2v_0 + \tfrac{4}{3}\mathscr{Q} = 0 . \tag{25}$$

In any case both conditions taken jointly make the solution unique.

It is worth emphasizing that assuring analyticity to the metric at the horizon has nothing to do with removing either strong or conical singularities from curvature invariants, since the vacuum between the core and the shell is free from strong singularities, whereas the conical ones are removable from there through conditions (14) and (15) above. Second, however Kruskal coordinates are historically linked to the question of geodesic completeness, this issue is not necessary to our purposes. In fact, we use here the analyticity of the Kruskal coordinates near the horizon of the central black hole only to assure that the shell is a *truly* controllable perturbation of the black hole in that region if expanded at any truncation order in the shell parameters, in the same sense considered by Vishveshwara (1970) for linear perturbations. Relations (24) and (25) show that analyticity near the horizon is a nontrivial property of the relativistic shells, having to be forced into the solution to assure its analytic behavior there.

### 2.3. *The Linearized Model: Conical Singularities and the Regge-Wheeler Formalism*

We consider now the linearization of the solution with respect to the shell parameters, i.e., we consider the shell as a small perturbation (e.g., formed by dust) of the central black hole geometry. Owing to the spherical symmetry of the Schwarzschild background, it is assumed that *any* linear perturbation could be expanded in spherical harmonics, an approach due primarily

to Regge & Wheeler (1957) to study the stability of black holes under small perturbations. We shall see that this is not true if conical singularities are present, in spite of the fact that the perturbation we are dealing with is a perfectly linear one.

We first summarize the Regge-Wheeler approach. The metric is expanded as $g_{\mu\nu} = g^S_{\mu\nu} + \epsilon h_{\mu\nu} + O(\epsilon^2)$, where $g^S_{\mu\nu}$ is the Schwarzschild metric, $\epsilon$ is some small parameter, and $h_{\mu\nu}$ is the general first-order perturbation of the metric. We put $g_{\mu\nu}$ in the Einstein vacuum equations $\mathfrak{R}_{\mu\nu} = 0$, where $\mathfrak{R}_{\mu\nu}$ is the Ricci tensor, and obtain $\mathfrak{R}_{\mu\nu} = 0 + \epsilon R_{\mu\nu} + O(\epsilon^2) = 0$, which leads to the well-known Regge-Wheeler (RW) differential equations $\epsilon R_{\mu\nu} = 0$ for the perturbation $\epsilon h_{\mu\nu}$. Before trying to solve these equations, it is possible to expand $\epsilon h_{\mu\nu}$ in tensor spherical harmonics in the Schwarzschild coordinates $(t, R, \theta, \phi)$ (see Mathews 1962; Zerilli 1970; Thorne 1980). $\epsilon h_{\mu\nu}$ falls in one of the two following general classes of perturbations, depending on its parity under rotations about the origin performed on the two-dimensional manifold $t = \text{const}$, $R = \text{const}$: one class (the even-type one) has parity $(-1)^\ell$ and its general (symmetric) form is

$$\epsilon h_{\mu\nu} = \begin{pmatrix} (1 - 2/R)H_0^{\ell m} & H_1^{\ell m} & h_0^{\ell m}\partial_\theta & h_0^{\ell m}\partial_\phi \\ H_1^{\ell m} & (1 - 2/R)^{-1}H_2^{\ell m} & h_1^{\ell m}\partial_\theta & h_1^{\ell m}\partial_\phi \\ h_0^{\ell m}\partial_\theta & h_1^{\ell m}\partial_\theta & R^2(K^{\ell m} + G^{\ell m}\partial_1) & R^2 G^{\ell m}\partial_2 \\ h_0^{\ell m}\partial_\phi & h_1^{\ell m}\partial_\phi & R^2 G^{\ell m}\partial_2 & R^2 \sin^2\theta(K^{\ell m} + G^{\ell m}\partial_3) \end{pmatrix} Y_{\ell m}\,, \tag{26}$$

where $Y_{\ell m}(\theta, \phi)$ is the standard $\ell$, $m$–mode spherical harmonic; $H_i^{\ell m}(t, R)$, $h_i^{\ell m}(t, R)$, $K^{\ell m}(t, R)$, and $G^{\ell m}(t, R)$ are the corresponding functions of the nonangular coordinates; and we define the partial differential operators $\partial_1 = \partial_{\theta\theta}$, $\partial_2 = \partial_{\theta\phi} - (\cos\theta/\sin\theta)\partial_\phi$, and $\partial_3 = (1/\sin^2\theta)\partial_{\phi\phi} + (\cos\theta/\sin\theta)\partial_\theta$.

The *odd* class has parity $(-1)^{\ell+1}$ and its general (symmetric) form is

$$\epsilon h_{\mu\nu} = \begin{pmatrix} 0 & 0 & -f_0^{\ell m}(1/\sin\theta)\partial_\phi & f_0^{\ell m}\sin\theta\partial_\theta \\ 0 & 0 & -f_1^{\ell m}(1/\sin\theta)\partial_\phi & f_1^{\ell m}\sin\theta\partial_\theta \\ -f_0^{\ell m}(1/\sin\theta)\partial_\phi & -f_1^{\ell m}(1/\sin\theta)\partial_\phi & f_2^{\ell m}\partial_4 & (1/2)f_2^{\ell m}\partial_5 \\ f_0^{\ell m}\sin\theta\partial_\theta & f_1^{\ell m}\sin\theta\partial_\theta & (1/2)f_2^{\ell m}\partial_5 & -f_2^{\ell m}\sin^2\theta\partial_4 \end{pmatrix} Y_{\ell m}\,, \tag{27}$$

where $f_i^{\ell m} = f_i^{\ell m}(t, R)$ and $\partial_4 = (1/\sin\theta)\partial_{\theta\phi} - (\cos\theta/\sin^2\theta)\partial_\phi$, and $\partial_5 = (1/\sin\theta)\partial_{\phi\phi} + \cos\theta\partial_\theta - \sin\theta\partial_{\theta\theta}$.

The superposition of perturbations is valid in the linearized theory, so in the matrices above we can assume the Einstein summation convention in the indices $\ell$, $m$ (truncated at the convenience) for the case of a more general multimode perturbation. We can simplify these matrices further by exploring the freedom to make arbitrary, first order in $\epsilon$, coordinate transformations around $(t, R, \theta, \phi)$. In particular, the matrices achieve their most simple or canonical forms in the so-called Regge-Wheeler infinitesimal gauge (Regge & Wheeler 1957). Nonetheless, we do not need to go to that gauge here.

If we linearize equation (18) in the shell strengths we obtain for the perturbation $\epsilon h_{\mu\nu}$

$$\epsilon h_{\mu\nu} = \begin{pmatrix} (1 - 2/R)P & 0 & 0 & 0 \\ 0 & (1 - 2/R)^{-1}(-Q + P) & 0 & 0 \\ 0 & 0 & R^2(-Q + P) & 0 \\ 0 & 0 & 0 & R^2\sin^2\theta P \end{pmatrix}, \tag{28}$$

with $P$ and $Q$ given, respectively, by equations (10) and (11) after dropping the second-order terms in the shell strengths appearing in those equations (remember that $u = R - 1$ and $v = \cos\theta$).

The linear perturbation (28) is a compulsory solution of the linearized equations $\epsilon R_{\mu\nu} = 0$, since it is the first-order term of the expansion of an exact solution of the full equations. Having in mind the axial symmetry of our static diagonal perturbation, an inspection of it shows that it is a superposition of even-type modes only. Then, it should be fitted by the matrix (26) with the terms $\ell = 0,1,2,3$ and $m = 0$ retained. We find that this fitting is impossible in general. In fact, the linearized solution (28) is a Regge-Wheeler perturbation only if it satisfies the following additional constraints (here $\kappa = 1$):

$$\gamma_0 = 0\,, \qquad \mathscr{D} + \tfrac{2}{5}\mathscr{O} = 0\,. \tag{29}$$

On the other hand, the RW formalism lies on a sound mathematical basis, namely, the multipole expansion theory (for a review with emphasis in general relativity; see Thorne 1980), so the reason for this drawback must have a physical origin. In fact, as shown in Sokolov & Starobinskii (1977), a curvature (and hence a Ricci) tensor proportional to a Dirac delta term centered at the symmetry axis corresponds to conical singularities. A certain energy-momentum tensor with this same structure (it does not matter here how exotic they should be) arises in Einstein's equations, and hence we do not have a true vacuum between the core and the shell, as supposed from the beginning of the RW formalism. By comparing equation (29) with the conditions (14) plus (15) with $\kappa = 1$ for Schwarzschild's metric, we see that the former amounts to ruling out the conical singularities from the linear approximation. In other words, conical singularities *survive* to the linearization and their presence is an obstruction to the application of the RW formalism. So, what is somewhat surprising in all this is that conical singularities strutting the model against its own gravity persist after the linearization, contrary to the loosely accepted idea that they should lie in the very nonlinear realm of general relativity.

### 2.4. *The Newtonian Limit of the Relativistic Models*

We now consider the Newtonian limit of the model (18) in the Schwarzschild coordinates $(t, R, \theta, \phi)$. We assume that there exists a region $D$ in the vacuum between the core's horizon and the shell where the conditions of weak gravitational field and slow motion of test particles occur. Then, Einstein's equations reduce in $D$ to Laplace's equation for the Newtonian potential $\Phi$, which relates to the metric $g_{\mu\nu}$ only through the temporal component as $g_{tt} = 1 + (2/c^2)\Phi$. The remaining components of the metric are irrelevant to this approximation.

Now, we consistently assume that $D$ is far away from the horizon, where the Schwarzschild coordinates approximate to the usual time plus the Euclidean spherical ones [we maintain the notation $(t, R, \theta, \phi)$ in the latter approximation]. Next, we pass to cylindrical coordinates $(t, r, z, \phi)$ via $z = R\cos\theta$, $r = R\sin\theta$ and expand the component $g_{tt}$ of equation (18) to the first order in $v_0$, $\mathscr{D}$, $\mathscr{Q}$, and $\mathscr{O}$, to obtain after some manipulation:

$$g_{tt} = 1 + \left(\frac{2}{c^2}\right)\Phi \equiv 1 + 2v_0 - \frac{2}{R} - \frac{4v_0}{R} + 2\mathscr{D}z\left(1 - \frac{2}{R}\right)\left(1 - \frac{1}{R}\right) + \mathscr{Q}(2z^2 - r^2)\left(1 - \frac{2}{R}\right)\left[\left(1 - \frac{1}{R}\right)^2 - \frac{1}{3R^2}\right]$$
$$+ \mathscr{O}(2z^3 - 3zr^2)\left(1 - \frac{2}{R}\right)\left(1 - \frac{1}{R}\right)\left(1 - \frac{2}{R} + \frac{2}{5R^2}\right). \tag{30}$$

The equation above was presented in VL1 (without the dipole) in a rather obscure (yet correct) form for the sake of obtaining the Newtonian limit. By assumption, the nondimensional constants satisfy $|v_0, \mathscr{D}, \mathscr{Q}, \mathscr{O}| \ll 1$; moreover, $R$ satisfies $R \gg 2$ in the region $D$, so that the only place where $R$ itself survives is in the term $2/R$ of equation (30), just that due to the monopolar core with mass $M$. The final step is to rewrite the surviving terms with the unit of length $L = GM/c^2$ appearing explicitly (remember that until now $R$ stood for $R/L$, etc.). The result for $\Phi$ is

$$\Phi = c^2 v_0 - \frac{GM}{R} + \frac{\mathscr{D}c^2}{L}\,z + \frac{\mathscr{Q}c^2}{2L^2}\,(2z^2 - r^2) + \frac{\mathscr{O}c^2}{2L^3}\,(2z^3 - 3zr^2)\,. \tag{31}$$

For comparison, let us briefly recall ab initio the proper Newtonian formulation: let the coordinate origin stay at the center of mass of the monopolar core (with mass $M$), let $z$ be the symmetry axis of the core-shell system, and let $D_N$ be the region between the smallest and the largest spheres centered at the origin that isolate the inner vacuum from the core and the shell. We have to solve Laplace's equation in $D_N$ for the axially symmetric Newtonian potential. By using the standard Legendre expansion, we arrive at the following gravitational potential $\Phi_N$ felt by test particles evolving in $D_N$:

$$\Phi_N = -\frac{GM}{R} - G\left[I_0 + I_1\,z + \frac{1}{2}\,I_2(2z^2 - r^2) + \frac{1}{2}\,I_3(2z^3 - 3zr^2) + \cdots\right], \tag{32}$$

where $R^2 = r^2 + z^2 = x^2 + y^2 + z^2$ and $x, y, z$ are the usual Cartesian coordinates. $I_0, I_1, I_2, I_3$ are, respectively, the constant, dipole, quadrupole, and octopole shell strengths given by the following volume integrals over the shell with mass distribution $\rho(R, \theta)$ ($P_n$ denotes the Legendre polynomial of order $n$):

$$I_n = \int\int\int_{\text{shell}} \rho(R, \theta)\,\frac{P_n(\cos\theta)}{R^{n+1}}\,dV\,. \tag{33}$$

Obviously, the regions $D$ and $D_N$ above must have a nonempty intersection if the Newtonian approximation to the full relativistic case is valid, so we assume this and compare both expressions (31) and (32) for the potential in $D \cap D_N$, thus obtaining

$$\left|v_0 = -\frac{m}{M} \times L\,\frac{I_0}{m}\right| \ll 1\,,$$
$$\left|\mathscr{D} = -\frac{m}{M} \times L^2\,\frac{I_1}{m}\right| \ll 1\,,$$
$$\left|\mathscr{Q} = -\frac{m}{M} \times L^3\,\frac{I_2}{m}\right| \ll 1\,,$$
$$\left|\mathscr{O} = -\frac{m}{M} \times L^4\,\frac{I_3}{m}\right| \ll 1\,, \tag{34}$$

where $m$ is the mass of the shell.

The question is "For which Newtonian shells are these constraints on the constants $I_n$ attainable?" To exemplify, let the shell be a homogeneous ring of mass $m$, radius $a$, and centered on the $z$-axis at $z = b$, whose density in cylindrical coordinates is $\rho = (m/2\pi a)\delta(r - a)\delta(z - b)$. The integrals $I_n$ in this case are

$$\frac{I_0}{m} = (a^2 + b^2)^{-1/2} = a^{-1}\left(1 + \frac{b^2}{a^2}\right)^{-1/2},$$
$$\frac{I_1}{m} = b(a^2 + b^2)^{-3/2} = ba^{-3}\left(1 + \frac{b^2}{a^2}\right)^{-3/2},$$
$$\frac{I_2}{m} = \frac{1}{2}\,(2b^2 - a^2)(a^2 + b^2)^{-5/2} = -\frac{1}{2}\,a^{-3}\left(1 - \frac{2b^2}{a^2}\right)\left(1 + \frac{b^2}{a^2}\right)^{-5/2},$$
$$\frac{I_3}{m} = \frac{1}{2}\,(2b^3 - 3a^2b)(a^2 + b^2)^{-7/2} = -\frac{1}{2}\,ba^{-5}\left(3 - \frac{2b^2}{a^2}\right)\left(1 + \frac{b^2}{a^2}\right)^{-7/2}. \tag{35}$$

In the limit $a \to 0$ the ring reduces to a particle with mass $m$ placed at $z = b$, whereas if $b \to 0$ it reduces to a ring placed at the equatorial plane with vanishing odd multipoles. In the case of $m/M \leq 1$, and given the characteristic core length $L = GM/c^2$ (a relativistic parameter we know, but that can be crudely anticipated already in the Newtonian frame by assuming light can be trapped by gravity like ordinary matter), we see that all constraints in equation (34) are satisfied for, say, $a \gg |b|, L$ (for the limiting case of a point particle at $z = b$, we let $a \to 0$ and this condition become $|b| \gg L$). Although intuitively expected, this enlightening example realizes the criteria to overlap both theories, that is to say, to assure the validity of the assumption $D \cap D_N \neq \emptyset$, and should be compared to the treatment made, for example, in Perry & Bohun (1992) for Weyl's solutions with usual, decreasing core-type multipoles.

We discuss now the physical role played by the constant $v_0$ in the model. Obviously, $v = v_0$, $\gamma = \gamma_0$ in equation (1) is a solution of equations (2) and (3) for any values of the constants $v_0, \gamma_0$. By the preceding discussion, its Newtonian limit leads to the constant potential $\Phi_N = c^2 v_0 = -GI_0$. What is the physical meaning of a constant Newtonian potential? It describes either trivially the empty space or rather the interior of a very special class of matter distributions, the so-called homoeoids (see Chandrasekhar 1987 and Binney & Tremaine 1987). The value of the constant potential inside a homoeoid is *not* arbitrary; its value is fixed by continuity requirements of the potential through the mass distribution of the homoeoid. Homoeoids are thus gravitationally undetectable from inside. This shows that the constant solution above is a strutted, relativistic version of a Newtonian homoeoid. If in addition we remove the conical singularity from inside the relativistic homoeoid by letting $\gamma_0 = 0$ (remember that conical singularities are not globally removable in static relativistic shell solutions, since they are indispensable to strut the shell against its own gravity, so $\gamma_0 = 0$ really moves them outside the shell), we see that a simple rescaling of the time and the radial coordinate reduces the metric inside the homoeoid to that of Minkowski. On the other hand, the condition (24) with $\mathscr{D} = \mathscr{Q} = \mathscr{O} = 0$ shows that if we add a black hole inside a homoeoid then the metric does not extend analytically through the black hole horizon *unless* we maintain the "strut" in place with strength $\gamma_0 = 2v_0$. This is a nonintuitive aspect of the (relativistic) composition of a black hole with the rather simple homoeoidal shell.

An easy point that is worth emphasizing concerning the interpretation of multipolar expansions of core and shell types is the following: core multipoles measure deviations from *sphericity* of central mass distributions, whereas shell multipoles measure how much shells deviate from *homoeoids*, the latter being a rather large class of distributions in which homogeneous spherical shells are very particular members.

We close this section with a brief discussion about the Hénon-Heiles structure of the present Newtonian limit. It was already pointed out in VL1 that the potential of the shell alone pertains to the Hénon-Heiles family of potentials, yet it does not suffice from its own to confine orbits in the intermediate vacuum (see the opposite signs of $r$ and $z$ in the quadrupole term of eq. [31]). Although in practice we need to consider the full potential of a given galactic model, viz., its effective potential $\Phi_{\text{eff}}$. The Hamiltonian $H$ of a test particle with mass $\mu$ is given in this case by

$$H = \frac{1}{2\mu}(p_r^2 + p_z^2) + \mu\Phi_{\text{eff}} ,$$

$$\Phi_{\text{eff}} = \frac{1}{2}\left(\frac{\ell}{\mu r}\right)^2 + \Phi_N , \tag{36}$$

where $\ell$ is the conserved angular momentum of the particle associated with the axial symmetry of the galaxy (Binney & Tremaine 1987). It is also usual to assume that galaxies have further a reflection symmetry about an equatorial plane, in which case the motion restricted to that plane is integrable, in particular having a central stable circular orbit at some fixed radius, say, $r = r_0$. To study a nonplanar stellar orbit as a small deviation from the planar one, we perform a series expansion of $\Phi_{\text{eff}}$ in the variables $(r - r_0, z)$, thus approximating the full motion by a bidimensional harmonic oscillator perturbed by higher order terms. This is the very astronomical origin (after truncating the series and idealizing the numeric coefficients) of the cubic Hénon-Heiles polynomial, now a paradigm of nonintegrable potential. Some history about this potential in astronomy can be traced, for example, from Contopoulos (1960), Barbanis (1962), van de Hulst (1962), Ollongren (1962), and Hénon & Heiles (1964).

By adding the other terms to the terms originated from the shell expansion to form $\Phi_{\text{eff}}$, we are able to confine test motions in the intermediate vacuum around the central stable orbit. If the galaxy does not have reflection symmetry around a middle plane ($I_1, I_3 \neq 0$ in the Newtonian case and $\mathscr{D}, \mathscr{O} \neq 0$ in the relativistic one), planar central stable orbits are not possible, only stable orbits of distorted, nonplanar type remain. We will return in § 3 to the discussion of the implications for orbit regularity of the largely assumed hypothesis of reflection symmetry about middle planes in galaxy modeling.

## 3. NUMERICAL RESULTS: REFLECTION SYMMETRY AND CHAOTIC MOTION IN RELATIVISTIC AND NEWTONIAN CORE-SHELL MODELS

We study the chaotic behavior of orbits in the intermediate vacuum of Newtonian static axially symmetric core-shell models and then compare them to the geodesics of the corresponding relativistic cases. It is amazing that this class of models has relativistic and Newtonian counterparts to be compared; there are even sound observational motivations for both.

Specifically, we analyze in both cases the role played by a *discrete* symmetry, namely, the reflection symmetry around the equatorial plane, in regularizing orbits against chaotic behavior. The hypothesis of reflection symmetry is a widely spread assumption in astronomical modeling, and its twofold justification lies primarily in that too many real objects to be modeled seem in fact nearly symmetric with respect to a plane. On the other hand, the models are simplified in both analytical and numerical aspects by that assumption. Of course, we do not expect that symmetry be realized in nature exactly, so it is relevant to search for possible orbital effects of its breaking. It is important to realize that all cases treated here preserve the

axial symmetry—the next continuous symmetry after the missing spherical one, which allows us to isolate the dynamical effects of only breaking or preserving the reflection symmetry itself.

Another advantage of the present study is that it is model independent (of course within the class of models we are dealing with) as we are focusing on general multipolar shell expansions instead of on specific mass distributions.

All is made nondimensional again in this section by formally taking $\Phi_N \leftrightarrow \Phi_N/c^2$, $R \leftrightarrow R/L$, etc., $H \leftrightarrow H/(\mu c^2)$, $p_z \leftrightarrow p_z/(\mu c)$, etc., and $\ell \leftrightarrow \ell/(\mu c L)$ in equations (31)–(32) plus (36), such that the Newtonian system we consider comes from the Hamiltonian ($R^2 = r^2 + z^2$)

$$H = \frac{1}{2}(p_r^2 + p_z^2) + \frac{1}{2}\frac{\ell^2}{r^2} - \frac{1}{R} + \mathcal{D}z + \frac{1}{2}\mathcal{Q}(2z^2 - r^2) + \frac{1}{2}\mathcal{O}(2z^3 - 3zr^2)\,. \tag{37}$$

On the other hand, the geodesic system comes from the Lagrangean $\mathcal{L} \leftrightarrow \mathcal{L}/(\mu c)$ given by

$$\mathcal{L} = \tfrac{1}{2} g_{\alpha\beta}\,\dot{x}^\alpha \dot{x}^\beta\,, \tag{38}$$

where the metric tensor $g_{\alpha\beta}$ and the coordinates $x^0 = t$, $x^1 = \rho$, $x^2 = z$, $x^3 = \phi$ are obtained from the nondimensional invariant interval (1), and the dot represents the derivative $d/ds$. The proper definition of timelike geodesics out of the metric interval furnishes the first constant of motion $\mathcal{L} = \frac{1}{2}$. The Euler-Lagrange formulation of the geodesic equations is

$$\frac{d}{ds}\frac{\partial \mathcal{L}}{\partial \dot{x}^\mu} - \frac{\partial \mathcal{L}}{\partial x^\mu} = 0\,, \tag{39}$$

from which the two additional constants of motion associated with the static nature and axiality of the relativistic system are read out, namely, the relativistic energy $h$ and angular momentum $l$ defined by

$$h \equiv \frac{\partial \mathcal{L}}{\partial \dot{t}} = g_{tt}\,\dot{t}\,,$$

$$l \equiv \frac{\partial \mathcal{L}}{\partial \dot{\phi}} = g_{\phi\phi}\,\dot{\phi}\,. \tag{40}$$

The remaining two equations in (39) describe the dynamics for the variables $\rho$, $z$. We note that these $\rho$, $z$ are Weyl's coordinates. From equation (5) we see that whenever the Schwarzschild coordinate $R$ satisfies $R \gg 2$ it approximates the usual radial spherical one (denoted here by the same letter $R$), and the Weyl $\rho$, $z$ approximate the usual cylindrical ones $r$, $z$. We remember also that in the Newtonian limit $dt/ds \approx 1/g_{tt}^{1/2}$ (low velocities), $g_{tt} \approx 1 + 2\Phi_N/c^2$, so the relativistic energy $h$ and the Newtonian energy $E \leftrightarrow \mu\Phi_N/(\mu c^2)$ of an orbiting particle with mass $\mu$ are related through $h \approx 1 + E$, and the corresponding angular momenta are related through $l \approx \ell$. We put $v_0 = 0$ and $\kappa = 1$ in this section. We impose the conditions (14) and (15) for the absence of conical singularities on all running relativistic situations presented below, except of course for the purely dipolar shell. All Newtonian, as well as relativistic, Poincaré sections (surfaces of section) shown here are made at the plane $z = 0$ (with the appropriate coordinate interpretation in each case).

In Figure 1 we present typical effective Newtonian potential wells for the bounded orbits we are considering ($U$ denotes $\Phi_{\rm eff}$, and the positive parts of the potential surfaces surrounding the wells are cut). Figures 1*a* and 1*c* show cases of oblate and prolate potentials, respectively, both possessing reflection symmetry about the equatorial plane given by $z = 0$. Oblate cases (Fig. 1*a*) have positive quadrupole strengths ($\mathcal{Q} > 0$), whereas prolate cases (Fig. 1*c*) have $\mathcal{Q} < 0$ (respectively, $I_2 < 0$ and $I_2 > 0$; see eqs. [31] and [32] and, for the specific case of a ring, eq. [35]). The presence of the reflection symmetry implies the vanishing of all odd shell multipoles ($\mathcal{D}$, $\mathcal{O}$, and $I_1$, $I_3$ here). We see that the oblate case has only one unstable equilibrium point (in the equatorial plane), whereas the prolate case has two of them (symmetrically placed outside the equatorial plane), which is easy to understand in terms of the exterior oblate/prolate shell mass distributions. Figures 1*b* and 1*d* show the typical deformation of the previous oblate and prolate cases, respectively, when we break the symmetry of reflection about $z = 0$ by introducing nonvanishing odd shell multipoles ($\mathcal{D}$, $\mathcal{O}$).

On the other hand, the relativistic regime is felt in the situation we are concerned with mainly through the existence of one more unstable equatorial equilibrium point in addition to those already present in the Newtonian potential. This intrinsically relativistic additional unstable point is associated with the presence of the black hole at the center and marks the point above which the orbits fall into the black hole. In the remaining, the relativistic potentials are qualitatively similar to those displayed in Figure 1 for the Newtonian case.

We have made a wider exploration of the shell parameters, energy, and angular momentum than shown here, with largely the same conclusions. The parameter values we actually chose to show are a compromise between the need to make consistent comparisons and the sharpening of the effects we found.

The case of a purely dipolar shell has been anticipated in VL2, where we stressed that the monopolar core plus shell dipole is nontrivial already in the Newtonian context. Moreover, we show that the Newtonian case is integrable whereas the relativistic one is chaotic, which justifies the characterization of chaos in the purely dipolar case as an intrinsic general relativistic effect. Here, we explore the fact that the Newtonian dipolar shell breaks the reflection symmetry of the model without breaking the integrability of the motion itself. Thus core-shell models provide us with two very distinct integrable situations from the point of view of the reflection symmetry: core plus dipolar shells (D cases), which do not have that symmetry, and purely monopolar cores (Keplerian cases), which do have it. A typical Poincaré section of an integrable D case is shown in Figure 2*a*.

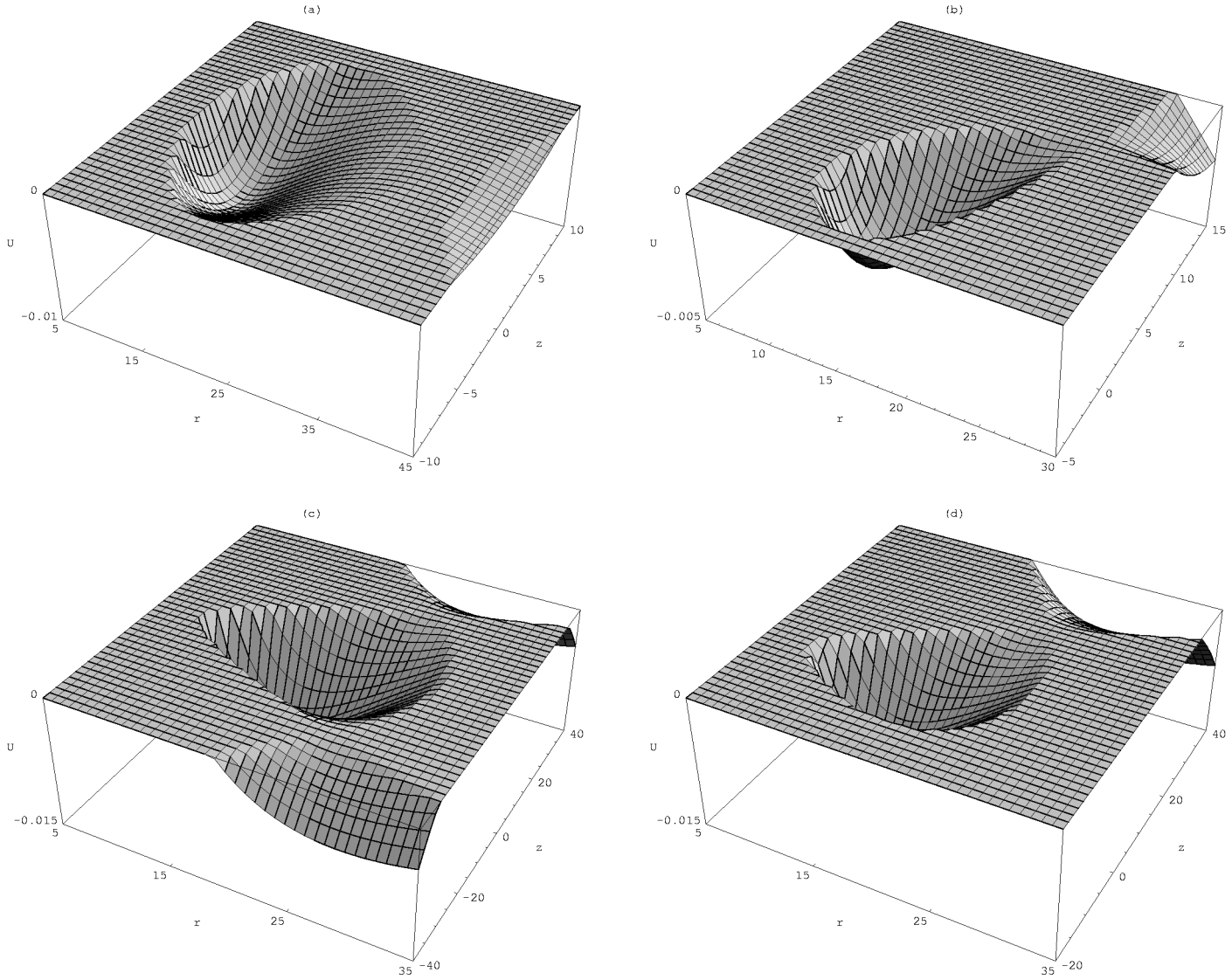


FIG. 1.—Typical effective Newtonian potential wells. $U$ denotes $\Phi_{\rm eff}$ and the positive parts of the full potential surfaces are cut. (*a*) Even ($\mathscr{D} = \mathscr{O} = 0$) oblate ($\mathscr{Q} > 0$) shell. (*b*) Oblate shell's perturbation due to the presence of the odd shell multipoles $\mathscr{D}$ and/or $\mathscr{O}$. (*c*) Even prolate ($\mathscr{Q} < 0$) shell. (*d*) Prolate shell's perturbation due to the presence of the odd shell multipoles. Note that (*a*) and (*c*) have a plane of symmetry, which is broken by the odd multipoles in (*b*) and (*d*).

First, we perturb both integrable configurations above with a reflection symmetry preserving, *oblate* quadrupolar term ($\mathscr{Q} > 0$). Surfaces of section for core plus oblate quadrupolar shells (oblate Q cases) are shown in Figures 2*b*, 2*c*, and 2*f*, whereas sections for core plus oblate dipolar-quadrupolar shells (oblate DQ cases) are shown in Figures 2*d* and 2*e*. These figures show that the breaking of the integrability of the D cases (without reflection symmetry) by a quadrupole is much stronger than that of the Keplerian case (with reflection symmetry) by the same quadrupole. Moreover, Figure 2*c* shows that chaotic behavior in the oblate Q cases is in fact present only in a residual, "microscopic" level, Figure 2*f* illustrates the robustness of the strong regularity of the oblate Q cases against the varying of the quadrupole strength, whereas Figure 2*e* shows that the strong chaotic behavior in the DQ cases is very dependent on the energy, in contrast with the robustness of the almost regularity of the oblate Q cases also with the energy.

Figure 3 shows the effects of introducing a reflection symmetry breaking, octopolar perturbation on the two integrable configurations (D cases and Keplerian cases), and also on the almost regular oblate Q cases. Figures 3*a* and 3*f* show the effects of a purely octopolar shell on the Keplerian case (O case) at two different octopole strengths. We see that these effects are very much stronger in comparison with the almost regular oblate Q cases. Figures 3*b*–3*e* show the effects of the various combinations of shell multipoles and confirm the dominance of the chaotic effects associated with the odd multipoles over those related to the purely oblate Q cases. In particular, the enhancement of chaotic behavior associated with the breakdown of the reflection symmetry is reinforced by the oblate QO cases presented in Figure 3*c* in comparison with the oblate Q cases, and Figures 3*d* and 3*e* confirm the strong dependence with the energy of the chaotic behavior associated with the lack of reflection symmetry.

Figure 4 shows surfaces of section for *prolate* quadrupolar cases ($\mathscr{Q} < 0$). Figures 4*a*–4*c* show the very much higher chaotic behavior of the prolate Q cases in comparison to the previous quasi-regular oblate Q cases. This is to be expected in view of

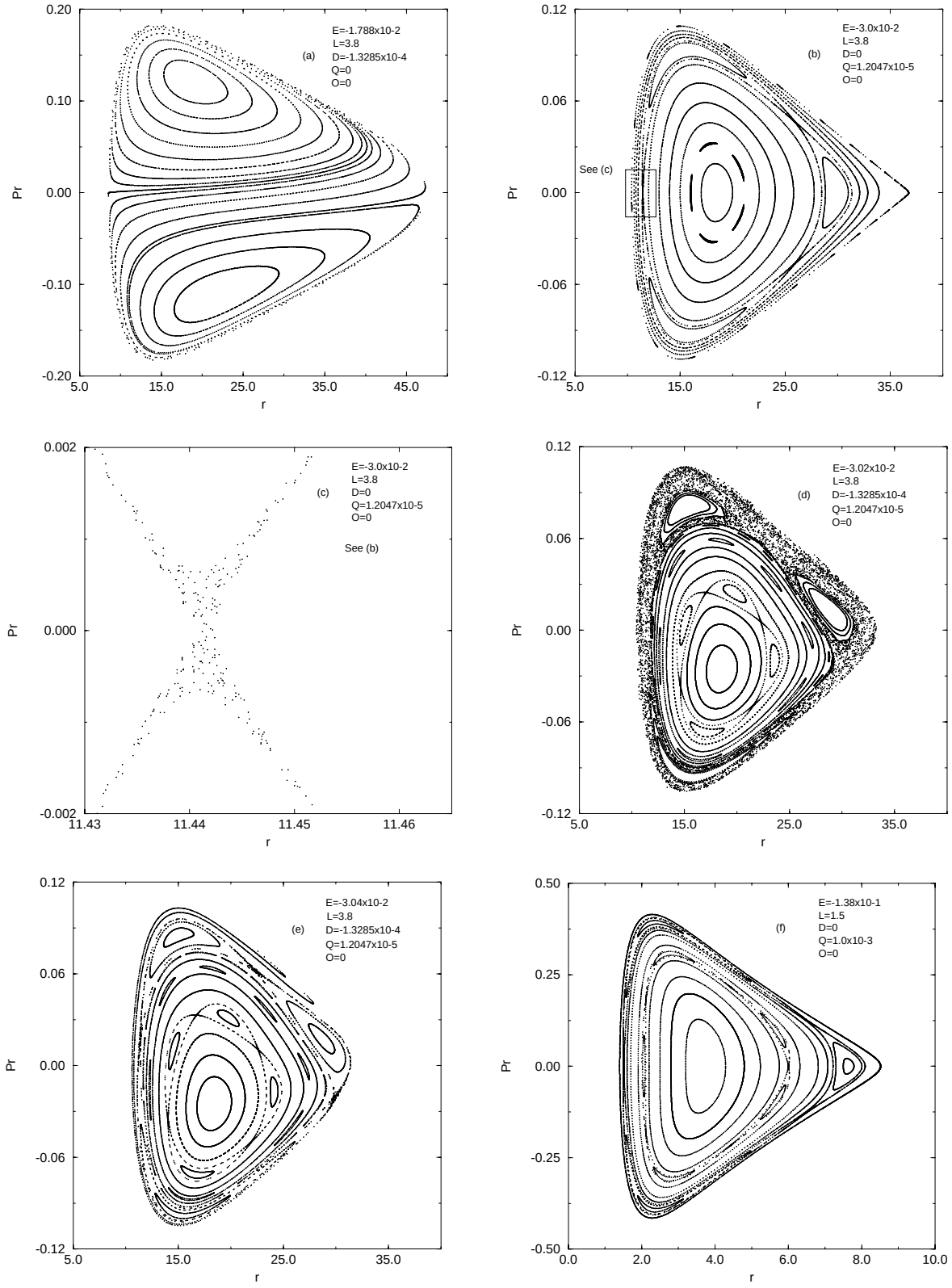


FIG. 2.—Surfaces of section at the plane $z = 0$ of integrable Newtonian configurations (D cases and Keplerian cases) perturbed by *oblate* shell quadrupoles only for the parameter values shown. Note that quadrupolar perturbations preserve the mirror symmetry. In all figures L accounts for the nondimensional angular momentum $\ell$. (*a*) Typical section of the integrable D case. This case does not have a plane of symmetry, in contrast with the also integrable spherically symmetric Keplerian case. (*b*), (*c*), and (*f*) Perturbed Keplerian cases (oblate Q cases). (*d*) and (*e*) Perturbed D cases (DQ cases). Note that orbit regularity is strongly broken (preserved) in the absence (presence) of mirror symmetry, this conclusion being robust against multipole strength variations.

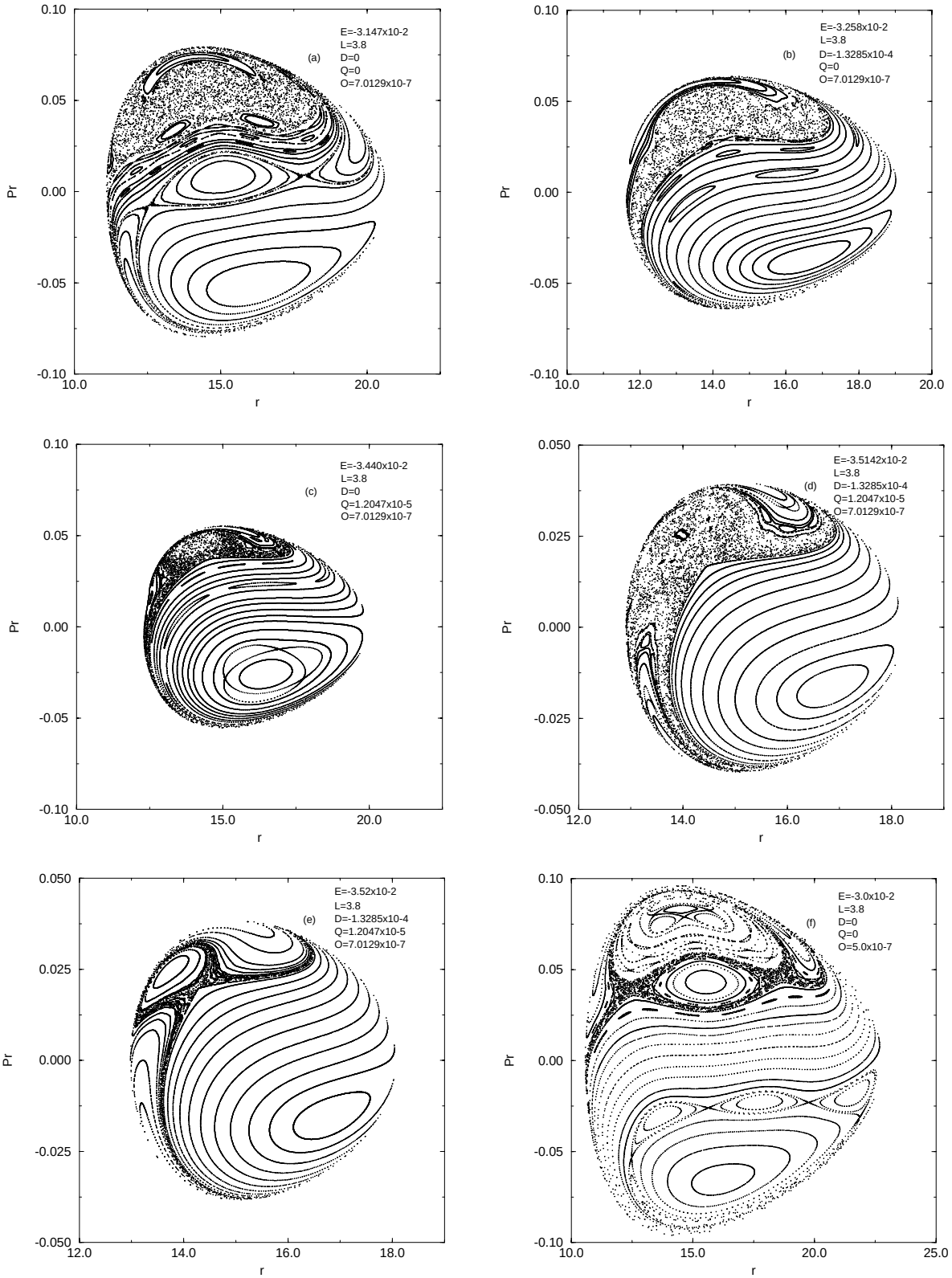


FIG. 3.—Octopolar components ($\mathcal{O} \neq 0$) added to the shell, necessarily breaking the mirror symmetry. (*a*) and (*f*) Strong chaotic effect of perturbing Keplerian cases with octopoles (O cases) (compare with the almost regularity of Figs. 1*b*, 1*c*, and 1*f*). (*b*) Strong chaotic effect of octopoles on integrable D cases (DO cases), which is fully expected as mirror symmetry is already absent from the starting. In (*c*) we break the reflection symmetry of the almost regular oblate Q case with octopoles (QO cases). (*d*) and (*e*) Full DQO case for two slightly different energies, which confirms the strong dependence of the chaotic behavior with the energy when the mirror symmetry is broken, in contrast with the robustness of the almost regular, mirror symmetric cases against energy variations.

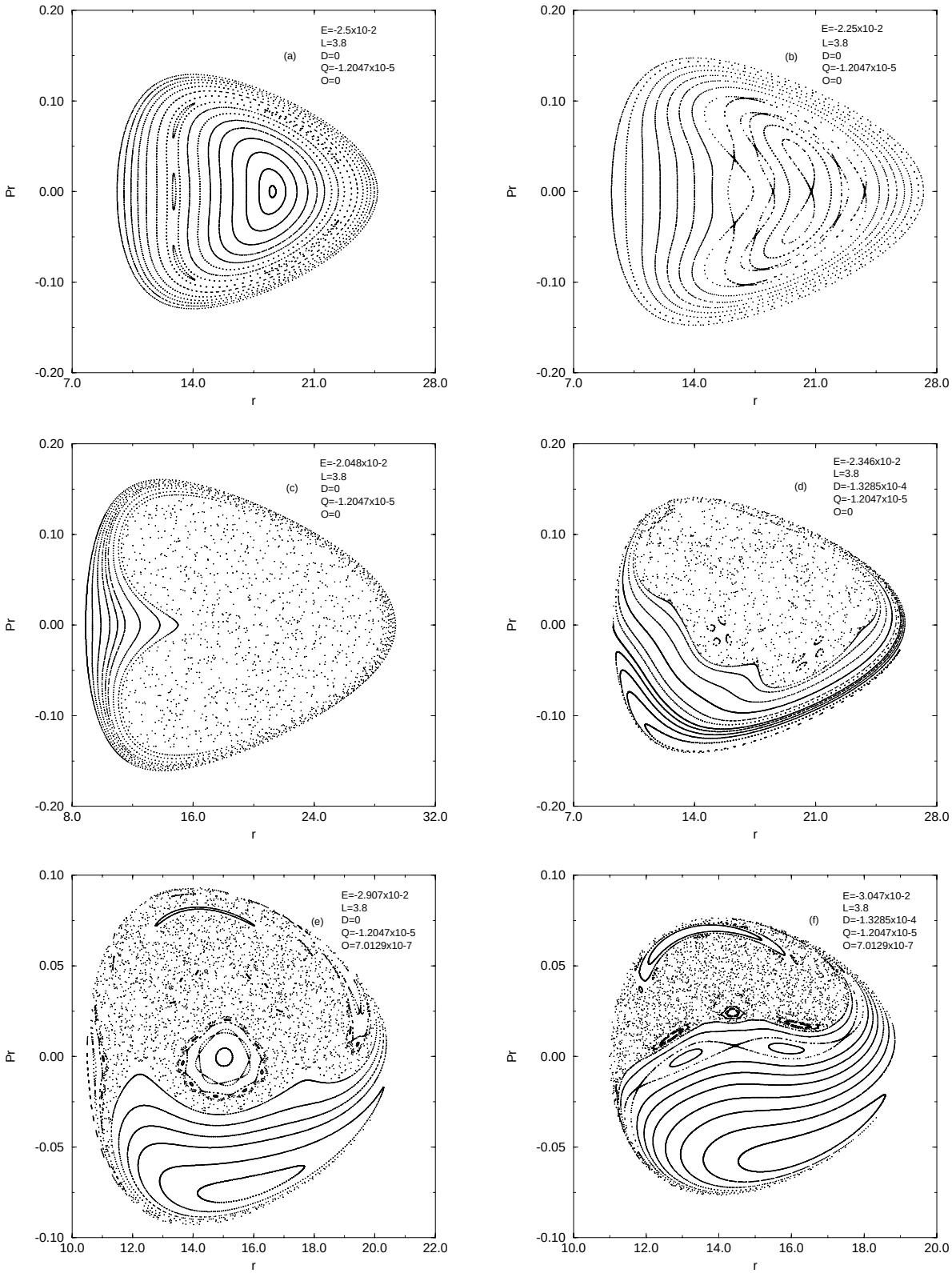


FIG. 4.—*Prolate* Q cases. (*a*)–(*c*) Illustration of the well-known fact that (mirror symmetric) prolate Q cases are strongly chaotic on their own and that their chaotic behavior is highly energy dependent. We note in particular that the orbit bifurcations toward the chaotic behavior unusually start from the central primary stable orbit itself rather than from the boundary. In (*d*)–(*f*) we break the mirror symmetry of the prolate Q cases with different combinations of odd multipoles. This causes a strong regularizing effect on the orbits, in particular by restoring, of course in a distorted fashion, the whole family of regular orbits around a primary stable orbit. Moreover, this restoration is robust against multipole strength, as well as energy variations.

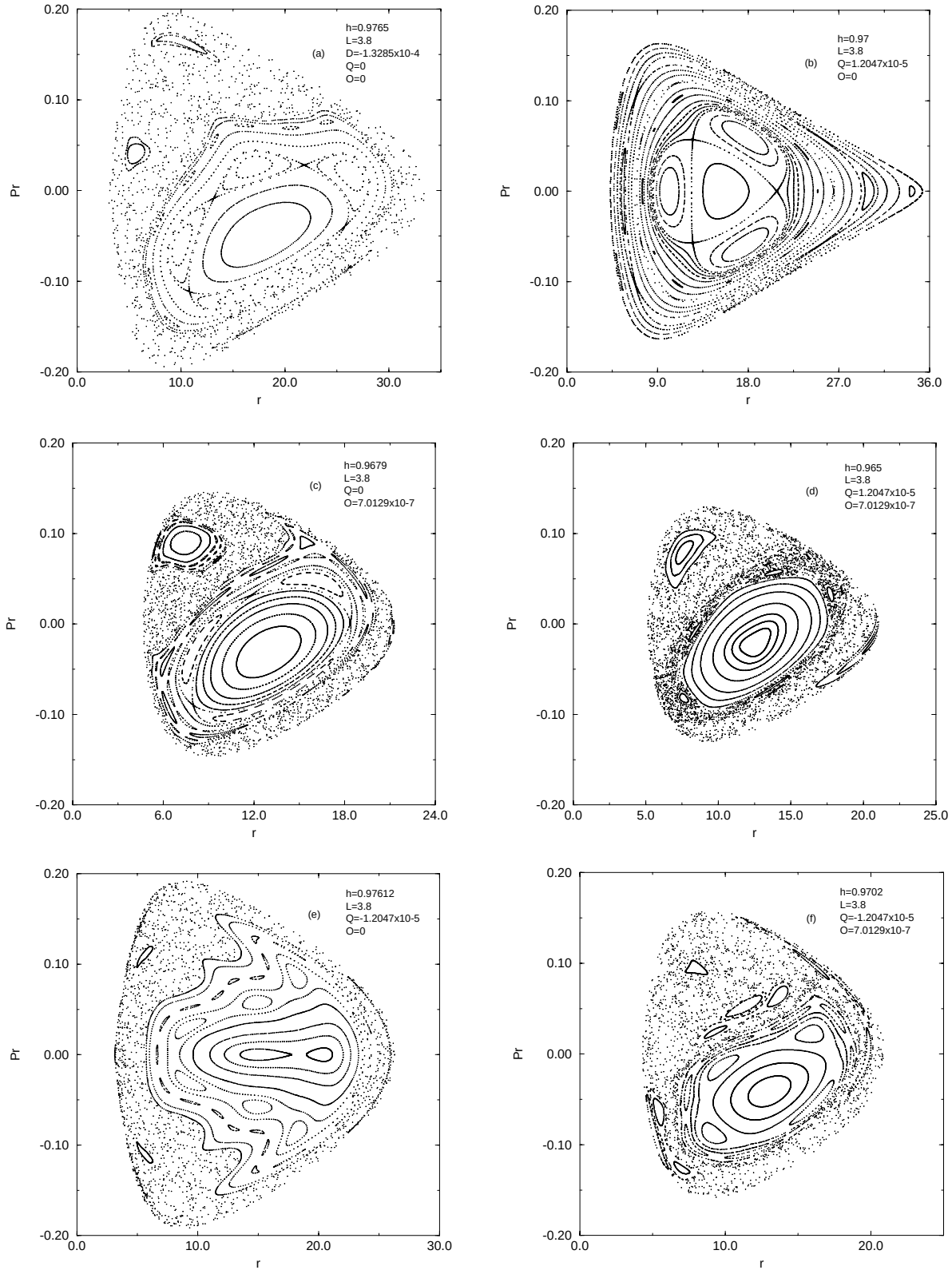


FIG. 5.—Some surfaces of section at the plane $z = 0$ for the corresponding fully relativistic core-shell configurations. The coordinates $r$, $z$ represent the Weyl ones $\rho$, $z$ (see text for more details). In addition, in ($a$) we set $v_0 = \gamma_0 = 0$ (in the purely dipolar case conical singularities [CSs] are unavoidable), whereas in ($b$)–($f$) we set $v_0 = 0$, and, in order to eliminate CSs, $\gamma_0$ and $\mathscr{D}$ are given in terms of $\mathscr{Q}$ and $\mathscr{O}$ according to the conditions (14) and (15). The relativistic case confirms the role of the presence/absence of the reflection symmetry on the chaotic behavior of the orbits already detected in the preceding Newtonian figures.

the prolate Q cases having two unstable equilibrium points (and hence suffering the simultaneous influence of the two corresponding instability regions) instead of only one occurring in the oblate Q cases. These figures also show that the central primary stable orbit, deeply inside the accessible region, is strikingly the first one to bifurcate and drive the chaotic behavior with the rising of the energy. The strong dependence with the energy of the whole set of bifurcations is also a distinctive aspect of these figures. In Figure 4*d* we show the effect of applying the perturbing prolate quadrupolar term on the integrable, reflection symmetry missing D cases (prolate DQ cases). We find that the absence of mirror symmetry in the prolate DQ cases causes the opposite to that occurring in the oblate DQ cases, namely, the missing mirror symmetry greatly enhances the orbit regularity in the prolate cases. Figure 4*e* confirms that the breakdown of mirror symmetry associated with the addition of an octopolar term to the prolate Q cases (prolate QO cases) strongly reduces the chaotic manifestation of the prolate Q cases themselves. In particular, Figures 4*d*–4*f* show evidence that the lack of symmetry introduces a robust family of regular asymmetric orbits around a stable primary one in the bounded region. This regularizing effect due to the lack of mirror symmetry in the prolate DQO cases is easily understandable in terms of the progressive lack of influence of one among the two unstable equilibrium points of the potential on the bounded region accessible to the particle if odd shell multipoles are put in scene (cf. Figs. 1*c* and 1*d*).

We present in Figure 5 the findings for the corresponding *relativistic* core-shell models. We choose for these figures the same nondimensional multipole shell strengths and angular momenta of the corresponding Newtonian figures and, except for the purely dipolar shell, we always eliminate the conical singularities (or "struts") from the intermediate vacuum by fixing $\gamma_0$ and $\mathscr{D}$ in terms of $\mathscr{Q}$ and $\mathscr{O}$ through the conditions (14) and (15). Also, we always put $v_0 = 0$ here. The relativistic energy $h$ is chosen in each case to be close to that given by the approximate relation $h \approx 1 + E$ where $E$ is the Newtonian energy.

Figure 5*a* shows a typical surface of section for a black hole plus purely dipolar shells (RD cases), where its strong chaotic behavior has to be compared with both the almost regularity of the *oblate* relativistic quadrupolar case (RQ case) shown in Figure 5*b* (its very small chaotic zones are visible if we zoom the cross-type regions between the islands) and the corresponding integrable Newtonian D case shown in Figure 2*a*. (In particular, the smallness of the chaotic zones of the oblate RQ case shown in VL1 occasioned the misleading statement made by us therein that these cases do not exhibit chaos, which was promptly corrected in Vieira & Letelier 1996b.)

In fact, Figure 5*b* does not represent the full chaotic behavior possible to oblate RQ cases. As we saw above regarding the relativistic counterparts of the Newtonian potentials, the relativistic oblate cases have one more unstable scape point (in fact, an infall point into the black hole) innermost at the equator in addition to that one provided in both cases by the oblate shell itself. Hence, if we vary the energy and the angular momentum so that both unstable regions are equally accessible by the bound nearly equatorial geodesics, it is possible to enhance strongly the chaotic behavior of Figure 5*b* to encompass even a significant portion of the more external region of the surface of the section (that associated with the nearly equatorial orbits). We will see more about this enhancement for the relativistic cases below in Figure 5*e*.

Figure 5*c* shows a surface of a section for relativistic dipolar-octopolar cases (RDO cases). Remember that both odd components are simultaneously needed in view of the off-strut constraint (15). Figure 5*d* is the same for full oblate RDQO cases. Figures 5*a*–5*d* show that the chaotic zones are greatly enlarged whenever odd shell multipoles are present, in contrast with the almost regular oblate RQ case shown.

Figure 5*e* shows a surface of section for relativistic *prolate* cases (prolate RQ cases). It is to be compared to the corresponding prolate Newtonian one (see Fig. 4*b*), in particular we note the evident fingerprints of the bifurcation series starting from the originally stable central primary orbit already present in the prolate Q cases. We also see that the prolate RQ cases share with the prolate Q cases the same relatively wild chaotic behavior as compared to the respective oblate (R)Q cases.

As in the Figure 5*b*, the dynamics would be more chaotic in Figure 5*e* if the angular momentum and the energy (unaltered here for the sake of full comparison) were adjusted to allow all three of the unstable points of the relativistic potential (instead of only the two related to the prolate character of the shell; see Fig. 1 and the comments therein about the additional black hole unstable point) to have stronger combined influence on the motion. So, the remaining differences between the relativistic Figure 5*e* and the Newtonian one (Fig. 4*b*) are due to the following: the central region (in the surface of section) is the only one able to become chaotic in the Newtonian case, since its orbits are just those (nonplanar ones) that can reach the unstable regions near the two unstable scape points symmetrically placed outside the equatorial plane, whereas the more external (in the surface of section) quasi-equatorial orbits are regular, since they are far from those two points and under the strong influence of the equatorial stable orbit in the boundary of the surface of section. When we change the Newtonian central mass by a true black hole then a third unstable scape point (in fact a rolling down point into the black hole) is placed innermost in the equatorial plane. There is one more unstable region associated with it that can be reached, this time by the quasi-equatorial orbits. The specific combination of parameters of Figure 5*e* is such that the central, nonplanar orbits can feel only moderately the influence of the two scape points linked to the presence of the prolate shell, whereas the quasi-equatorial orbits feel the nearby influence of the unstable point associated with the black hole strongly. As we said above, other combinations of parameters will allow a much stronger spread and eventually the overlapping of both types of chaotic regions.

Finally, Figure 5*f* shows the restoration of a robust set of regular asymmetric orbits around a primary stable one when we break the reflection symmetry around the equatorial plane by switching on the odd multipoles onto the prolate RQ cases, much the same as occurred in the prolate Newtonian Q cases.

## 4. DISCUSSION

In the first part of this article we presented a unifying discussion concerning the properties and, more important, the physical content of some relativistic, static, axially symmetric core-shell models on their own, as well as in connection with the corresponding linearized and Newtonian models taken as limiting cases. The analytical and observational motivations for

these relativistic and Newtonian models were also shown. This was accomplished in a reasonably self-contained manner in the introduction and § 2 and needs no additional comments.

In the second, numerical part of this work we explored the fact that the models (1) are generic within the class they pertain and (2) have exact relativistic and Newtonian counterparts to be compared, to study the chaotic behavior of bound orbits in the vacuum between the core and the shell.

Specifically, we first tested the relevance of the presence/absence of the reflection symmetry around the equatorial plane for the chaotic behavior of the orbits. We found consistent evidence for a nontrivial role played by the reflection symmetry on the chaotic behavior of the dynamics in both the relativistic and Newtonian cases. We summarize these findings as follows: the *breakdown* of the reflection symmetry about the equatorial plane in both Newtonian and relativistic core-shell models (1) *enhances* in a significant way the chaotic behavior of orbits in reflection symmetric *oblate* shell models and (2) *inhibits* significantly also the occurrence of chaos in reflection symmetric *prolate* shell models. In particular, the lack of the reflection symmetry provides the phase space in the prolate case with a robust family of regular orbits around a stable periodic orbit that is otherwise missing at higher energies.

The other point we addressed about the chaotic behavior of orbits was for the consequences of substituting true central black holes by Newtonian central masses. We find that the relative extents of the chaotic regions in the relativistic cases are significantly larger than in the corresponding Newtonian ones. Although not surprising in thesis, the strong differences between both regimes are in order in view of the procedure found in the literature of simulating the presence of a black hole at the core of a galaxy with a naive $-1/r$ Newtonian term (see, for example, Gerhard & Binney 1985; Sridhar & Touma 1997; Valluri & Merritt 1998). This approximation is certainly valid far from the black hole but not in its proximity, as is the case here.

These findings stress (1) the nontrivial role of the reflection symmetry in both relativistic and Newtonian regimes, in contrast with its universal acceptance in astronomical modeling, (2) the strong qualitative and quantitative differences between relativistic and Newtonian regimes, in particular when dealing with orbits in the vicinity of black holes, and (3) the intricate interplay between both aspects when they are simultaneously present.

The true dynamical aspect related to the role of reflection symmetries on the regularity of the orbits refers of course to the parity of the constants of motion (the famous third one in the present axially symmetric case) with respect to the coordinates, as well as their power to regularize orbits in phase space. Translated to these terms, the findings above are saying that the additional constant of motion in question is by far more powerful whenever (1) it is an *even* function of the coordinates for *oblate* cases, or (2) it is an *odd* function of the coordinates for *prolate* cases. Since the issue of finding global or even approximate constants of motion given the dynamics is hard if not feasible in most cases, the former procedure of simply checking the presence/absence of reflection symmetries is of much more practical interest.

Additional study is needed to see whether and how our findings are extendable to more realistic configurations, with and without black holes/central masses. The obvious improvement is to fill the intermediate vacuum with some reasonable mass distribution. Although this is far from obvious in general relativity, it is easy to do in the Newtonian context. For example, we are considering just superposing our shell multipoles to some relevant potentials of celestial mechanics such as Plummer-Kuzmin, Ferrers, and others and even triaxial potentials. They have one or more planes of symmetry, with or without axial symmetry, and so we can perturb them with shell terms to verify similar effects to those we found.

Here we considered only tube orbits ($l_z \neq 0$), since we are interested in the effects of the existence of planes of symmetry on *tridimensional* motion (somewhat similar effects to those found here are seen in Gerhard 1985 for the restricted case of planar motions with respect to the existence of one or more lines of symmetry). The model improvements above will allow us to study the effects of breaking the reflection symmetry also on tridimensional box orbits.

Meantime, the fully relativistic program is in progress. We have recently succeeded in giving rotation to a black hole (i.e., in converting it into a Kerr black hole) plus a dipolar shell term (Letelier & Vieira 1997). There is increasing evidence for the existence of black holes, particularly inside active galactic nuclei (Kormendy & Richstone 1995), which motivates us to consider also rotating core-shell models in the same lines followed here.

The authors thank FAPESP and CNPq for financial support and Jorge E. Horvath and Andre L. B. Ribeiro for discussions.

## REFERENCES

Araujo, M. E., Letelier, P. S., & Oliveira, S. R. 1998, Classical Quantum Gravity, 15, 3051
Arnaboldi, M., Capaccioli, M., Cappellaro, E., Held, E. V., & Sparke, L. 1993, A&A, 267, 21
Arnol'd, V. I. 1963a, Russ. Math. Surv., 18, 9
———. 1963b, Russ. Math. Surv., 18, 85
Barbanis, B. 1962, Z. Astrophys., 56, 56
Barlow, M. J., Drew, J. E., Meaburn, J., & Massey, R. M. 1994, MNRAS, 268, L29
Barnes, J. E. 1993, ApJ, 419, L17
Barnes, J. E., & Hernquist, L. 1992, ARA&A, 30, 705
Berry, M. V. 1978, in AIP Conf. Proc. 46, Topics in Nonlinear Dynamics, Ed. S. Jorna (New York: AIP), 16
Binney, J. 1982a, MNRAS, 201, 15
———. 1982b, MNRAS, 201, 1
Binney, J., & Spergel, D. 1982, ApJ, 252, 308
Binney, J., & Tremaine, S. 1987, Galactic Dynamics (Princeton: Princeton Univ. Press)
Carminati, J., & McLenaghan, R. G. 1991, J. Math. Phys., 32, 3135
Chandrasekhar, S. 1987, Ellipsoidal Figures of Equilibrium (New York: Dover)
Chevalier, R. A. 1997, Science, 276, 1374
Contopoulos, G. 1960, Z. Astrophys., 49, 273
de Zeeuw, T. 1985, MNRAS, 216, 273
de Zeeuw, T., Peletier, R., & Franx, M. 1986, MNRAS, 221, 1001
Dupraz, C., & Combes, F. 1987, A&A, 185, L1
Evans, N. W., Häfner, R. M., & de Zeeuw, T. 1997, MNRAS, 286, 315
Gerhard, O. E. 1985, A&A, 151, 279
Gerhard, O. E., & Binney, J. 1985, MNRAS, 216, 467
Groenewegen, M. A. T., Whitelock, P. A., Smith, C. H., & Kerschbaum, F. 1998, MNRAS, 293, 18
Hénon, M., & Heiles, C. 1964, AJ, 69, 73
Kolmogorov, A. N. 1954, Dokl. Akad. Nauk. SSSR, 98, 527
Kormendy, J., & Richstone, D. 1995, ARA&A, 33, 581
Letelier, P. S., & Oliveira, S. R. 1998, Classical Quantum Gravity, 15, 421
Letelier, P. S., & Vieira, W. M. 1997, Phys. Rev. D, 56, 8095

Lynden-Bell, D. 1962, MNRAS, 124, 95
Madsen, J. 1991, ApJ, 367, 507
Malin, D. F., & Carter, D. 1983, ApJ, 274, 534
Mathews, J. 1962, J. Soc. Indust. Appl. Math., 10, 768
Merritt, D. 1997, ApJ, 486, 102
Merritt, D., & Fridman, T. 1996, ApJ, 460, 136
Meyer, F. 1997, MNRAS, 285, L11
Moon, P., & Spencer, D. E. 1988, Field Theory Handbook (Berlin: Springer)
Moser, J. 1967, Math. Ann., 169, 136
Norman, C. A., Sellwood, J. A., & Hasan, H. 1996, ApJ, 462, 114
Ollongren, A. 1962, Bull. Astron. Inst. Netherlands, 16, 241
Panagia, N., Scuderi, S., Gilmozzi, R., Challis, P. M., Garnavich, P. M., & Kirshner, R. P. 1996, ApJ, 459, L17
Perry, G. P., & Bohun, C. S. 1992, Phys. Rev. D, 46, 1866
Poincaré, H. 1957, Les Méthodes Nouvelles de la Mécanique Céleste (New York: Dover), Vols. 1–3
Quinn, P. J. 1984, ApJ, 279, 596
Ralston, J. P., & Smith, L. L. 1991, ApJ, 367, 54
Regge, T., & Wheeler, J. A. 1957, Phys. Rev., 108, 1063
Reina, C., & Treves, A. 1976, Gen. Relativ. Gravitation, 7, 817
Reshetnikov, V., & Sotnikova, N. 1997, A&A, 325, 933
Richstone, D. O. 1982, ApJ, 252, 496
Robertson, H., & Noonan, T. 1968, Relativity and Cosmology (London: Saunders)
Sackett, P. D., & Sparke, L. S. 1990, ApJ, 361, 408
Schwarzschild, M. 1979, ApJ, 232, 236
———. 1993, ApJ, 409, 563
Sokolov, D. D., & Starobinskii, A. A. 1977, Soviet Phys. Dokl., 22, 312
Sridhar, S., & Touma, J. 1997, MNRAS, 287, L1
Suen, W.-M. 1986a, Phys. Rev. D, 34, 3617
———. 1986b, Phys. Rev. D, 34, 3633
Thorne, K. S. 1980, Rev. Mod. Phys., 52, 299
Valluri, M., & Merritt, D. 1998, ApJ, 506, 686
van de Hulst, H. C. 1962, Bull. Astron. Inst. Netherlands, 16, 235
Vieira, W. M., & Letelier, P. S. 1996a, Phys. Rev. Lett., 76, 1409 (VL1)
———. 1996b, Los Alamos Data Bank (gr-qc/9608030)
———. 1997, Phys. Lett. A, 228, 22 (VL2)
Vishveshwara, C. V. 1970, Phys. Rev. D, 1, 2870
Zerilli, F. J. 1970, Phys. Rev. D, 2, 2141
Zhang, X.-H. 1986, Phys. Rev. D, 34, 991